

Accelerating subglacial hydrology for ice sheet models with deep learning methods

Vincent Verjans¹, Alexander Robel¹

¹School of Earth and Atmospheric Sciences, Georgia Institute of Technology, Atlanta, GA, USA

Key Points:

- We develop a deep learning emulator to simulate evolving subglacial hydrology in response to meltwater input for ice sheet simulations.
- The emulator shows generalization capabilities, large computational savings, and can be used to force numerical ice sheet models.
- We demonstrate that machine learning has substantial potential in improving ice sheet models, through using information-rich data sets.

Corresponding author: Vincent Verjans, vverjans3@gatech.edu

Abstract

Subglacial drainage networks regulate the response of ice sheet flow to surface meltwater input to the subglacial environment. Simulating subglacial hydrology evolution is critical to projecting ice sheet sensitivity to climate, and contribution to sea-level change. However, current numerical subglacial hydrology models are computationally expensive, and, consequently, evolving subglacial hydrology is neglected in large-scale ice sheet simulations. We present a deep learning emulator of a state-of-the-art subglacial hydrology model, trained at multiple Greenland glaciers. Our emulator performs strongly in both temporal ($R^2 > 0.99$) and spatial ($R^2 > 0.96$) generalization, offers high computational savings, and can be used to force numerical ice sheet models. This will enable century- and large-scale ice sheet model simulations, including interactions between ice flow and increased meltwater input to the subglacial environment. Generally, our work demonstrates that machine learning can further improve ice sheet models, reduce computational bottlenecks, and exploit information from high-fidelity models and novel observational platforms.

Plain Language Summary

Meltwater at the surface of ice sheets can drain to the subglacial environment, lubricate the bed, and influence ice sheet flow. Complex numerical subglacial hydrology models represent the subglacial drainage system, but are too computationally expensive to be included in large-scale and long-term ice sheet simulations. Consequently, model predictions of future ice sheet contribution to sea-level rise ignore ice flow modulation by evolving subglacial hydrology. Here, we use deep learning to emulate a state-of-the-art subglacial hydrology model. The emulator can directly force large-scale ice sheet models to capture ice flow sensitivity to subglacial hydrology. The computational speed and accuracy of our emulator show the potential to use machine learning to efficiently incorporate previously neglected processes into ice sheet models.

1 Introduction

The Greenland ice sheet has experienced accelerating mass loss since the early 1990s (Otosaka et al., 2023). Ice loss has been driven by increasing surface melt (Fettweis et al., 2016) and accelerating ice flow into the ocean (King et al., 2020). These two processes are linked by surface meltwater drainage into the subglacial environment. The evolution of the subglacial drainage system in response to meltwater input determines the subglacial water pressure, which regulates the speed of ice sliding over the bed (Nienow et al., 2017). Observations have demonstrated a strong sensitivity of ice flow speed to meltwater supply to the bed on timescales ranging from days to months (Zwally et al., 2002; Shepherd et al., 2009; Smith et al., 2021). The subglacial drainage system modulates this sensitivity, and there is no simple relationship between meltwater forcing and ice flow speed, due to the complexities of subglacial hydrology (Bartholomew et al., 2011; van de Wal et al., 2015).

Subglacial hydrology models simulate the evolution of subglacial water pressure under different conditions of ice sheet geometry and meltwater input (Werder et al., 2013; de Fleurian et al., 2018). They represent the transient evolution of the subglacial drainage system, are highly complex, and require many parameters and substantial computational expense (Werder et al., 2013; Hoffman et al., 2016). When applied to individual Greenland glaciers, studies have shown that accurately representing the evolution of the subglacial hydrology system with such complex models is necessary to explain observed variability in ice flow (Hewitt, 2013; Hoffman et al., 2016; Ehrenfeucht et al., 2022). However, their computational expense prohibits long, ice sheet scale simulations. In contrast, simple first-order formulations of the growth and decay of subglacial water flux do exist, facilitating large-scale simulations (Kazmierczak et al., 2022). But these formulations

do not represent the different drainage components and assume a constant transmissivity. As such, they have critical limitations when considering high meltwater input scenarios, complex topographies, or reproducing realistic variability in subglacial hydrology and ice flow (de Fleurian et al., 2018).

Most subglacial hydrology models divide subglacial drainage into distributed and channelized systems (Schoof, 2010; Werder et al., 2013; de Fleurian et al., 2018). The former is typical of the early melt season, when the subglacial hydrology system is inefficient and water pressure increases strongly with meltwater supply. Later in the melt season, the system develops into a channelized system, efficiently evacuating meltwater, and causes water pressure to decrease with increasing meltwater input (Schoof, 2010; Bartholomew et al., 2011; Cowton et al., 2013). Ice flow variability is sensitive to the representation of, and transitions between different forms of drainage. Nevertheless, because of their computational expense, subglacial hydrology models are not included in model simulations at ice sheet scale (Goelzer et al., 2020; Seroussi et al., 2020). Consequently, current sea-level projections ignore a critical process regulating ice flow.

The climate modeling community has used machine learning techniques successfully to parameterize processes unresolved in coarse resolution global models (e.g., Brenowitz & Bretherton, 2018; Rasp et al., 2018). In particular, artificial neural networks (ANNs) are particularly powerful tools for parameterizing complex relationships between input and output variables, as they are capable of approximating any continuous function (the universal approximation theorem, Hornik et al., 1989). Furthermore, recent improvements in computational hardware, software, and optimization techniques have led to important ANN developments in multiple fields, including the Earth sciences (LeCun et al., 2015; Reichstein et al., 2019). Once trained, ANN models are computationally efficient, and ANNs have been used previously to emulate glacier flow models (Brinkerhoff et al., 2021; Jouvét et al., 2021). In this study, we use deep learning to enable representation of subglacial hydrology in large-scale ice sheet model simulations. Specifically, we develop an ANN emulator of the Glacier Drainage System model (GlaDS, Werder et al., 2013), an advanced and computationally expensive subglacial hydrology model. More generally, our work is a proof of concept for an important advancement in ice sheet modeling: we demonstrate that deep learning techniques can replace computationally-demanding or poorly constrained processes in large-scale ice sheet models.

2 Methods

We run GlaDS for 40 years at eight major Greenland glaciers (Petermann, Jakobshavn, Helheim, Kangerlussuaq, Humboldt, Koge Bugt, Russell, and Upernavik, see Fig. S1 for locations). The glacier geometries and ice flow velocities are taken from present-day observations (Joughin et al., 2017; Morlighem et al., 2017), and the meltwater runoff forcing from the 1970-2009 output of the diurnal Energy Balance Model (Krebs-Kanzow et al., 2020) (see Supporting Information). GlaDS simulates the evolution of the subglacial hydraulic potential, ϕ , in time and space by representing both channelized and distributed drainage. Accurate representation of ϕ in ice sheet models is critical, as it directly determines the subglacial water pressure, p_w . In turn, p_w determines the effective pressure at the ice-bed interface, N :

$$\begin{cases} N = p_{ice} - p_w \\ p_w = \phi - g\rho_w B \\ p_{ice} = g\rho_{ice}H_{ice} \end{cases}, \quad (1)$$

where p_{ice} is ice pressure [Pa], g is gravitational acceleration [m s^{-2}], H_{ice} is thickness of the above-lying ice column [m], B is bed elevation [m], and ρ_w and ρ_{ice} are water and ice density [kg m^{-3}], respectively. Critically, N [Pa] is a key variable in basal sliding laws

108 for ice flow (Budd et al., 1984; Hewitt, 2013). We run GlaDS at a 2-hourly time step to
 109 preserve numerical stability.

110 Dynamics of ϕ are governed by the amount of surface meltwater draining through
 111 the ice sheet to the bed, followed by the routing of the water through the subglacial sys-
 112 tem. The goal of our ANN is to predict ϕ based on ice sheet state and meltwater runoff
 113 forcing, such that our p_w emulation accounts for spatio-temporal evolution of subglacial
 114 hydrology. Specifically, our ANN uses as inputs ice thickness, ice velocities, bedrock to-
 115 pography, and meltwater runoff fields, as well as moulin locations where meltwater reaches
 116 the subglacial domain. All these variables are common variables, parameters, or inputs
 117 to typical ice sheet models. Similar to current subglacial hydrology models, our ANN
 118 is aimed at one-way coupling with ice sheet models, i.e., it needs to be run prior to the
 119 ice sheet model and the ANN output is subsequently used as a forcing to the ice sheet
 120 model. We discuss prospects for full two-way coupling in the *Discussion* section.

121 Our ANN is a convolutional neural network, based on the U-Net architecture (Ronneberger
 122 et al., 2015). Our ANN thus uses two-dimensional input fields, and outputs a two-dimensional
 123 ϕ field at any given time step (see Supporting Information). In total, the ANN has 259,953
 124 trainable parameters that are optimized such that ANN predictions of ϕ match train-
 125 ing targets with accuracy. We calibrate our ANN to the GlaDS 1975-2004 output at seven
 126 of the eight glaciers. We keep the last 5 years (2005-2009) of output at these seven glaciers
 127 as test data to evaluate the temporal generalization capabilities of the ANN. Further-
 128 more, we keep all the output of the eighth glacier for test data in order to evaluate the
 129 ANN spatial generalization capabilities. All the GlaDS output test data were totally un-
 130 seen by the deep learning algorithm or the authors during the calibration. The calibra-
 131 tion data are separated into training data, used to optimize the ANN parameters, and
 132 validation data, used to optimize hyperparameters and to avoid overfitting (see Support-
 133 ing Information). All the results presented in the next sections have been computed on
 134 the test data.

135 3 Results

136 3.1 Temporal Generalization Performance

137 To assess the ability of the ANN to reproduce GlaDS hydraulic potential (ϕ) fields,
 138 we start by comparing their respective outputs at the 7 calibration glaciers over the last
 139 5 years of simulations (2005-2009), which have not been used for the ANN training. Fig-
 140 ures 1a and 1b show for one of the calibration glaciers (Helheim glacier) that the mean
 141 ϕ field of the ANN over these 5 test years reproduces the spatial patterns of GlaDS out-
 142 put well. In particular, the ANN captures the radial patterns of high ϕ values and vari-
 143 ability centered at moulin locations, where meltwater runoff drains to the subglacial en-
 144 vironment. The ANN performs well throughout the domain, as the root-mean-square
 145 error (RMSE) is mostly lower than 0.5 MPa (Fig. 1c). The temporal dynamics are also
 146 captured well, as ϕ time series show close correspondence between ANN and GlaDS out-
 147 puts in most of the domain (Fig. 1d). The ANN captures the different ranges in season-
 148 ality and inter-annual variability of ϕ . It also reproduces the asymmetry between early
 149 and late melt season, which is due to changing drainage efficiency (Nienow et al., 2017).
 150 In Figure 1d, the orange curve shows a time series selected within the high RMSE area
 151 (Fig. 1c). This example illustrates that the ANN still captures the temporal variabil-
 152 ity, but is biased low at this particular location.

153 Figure 1e shows the ANN performance over the 5 years of test data at all the seven
 154 calibration glaciers, demonstrating low bias and RMSE. Furthermore, the ANN explains
 155 >99% of the variance in GlaDS ϕ output, as quantified by the coefficient of determina-
 156 tion (R^2). These results demonstrate that the ANN is able to predict ϕ with good ac-
 157 curacy over years, and thus meltwater input conditions, unseen during training.

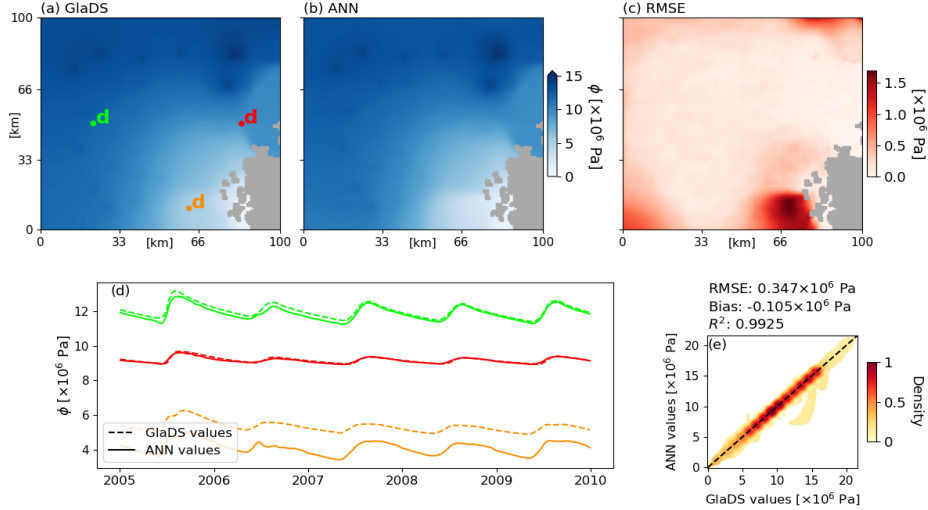


Figure 1. Temporal generalization performance of the ANN over the test period. Maps of mean 2005-2009 ϕ fields at one calibration glacier (Helheim, Fig. S1 for location) simulated by (a) GlaDS, and (b) the ANN. The Root-Mean-Square Error (RMSE) of the ANN with respect to GlaDS is shown in (c). Time series (d) of ϕ at specific grid points simulated by GlaDS (dashed lines) and the ANN (solid lines), with color-coded locations shown in (a). Performance statistics (e) of the ANN with respect to GlaDS evaluated at all the grid points of the 7 calibration glaciers for all the 2005-2009 time steps.

158

3.2 Spatial Generalization Performance

159

160

161

162

163

164

165

166

167

168

169

170

We now perform a similar evaluation, but at the test glacier (Upernavik), not included in the ANN calibration. This task presents a harder challenge, as both years of meltwater runoff and glaciological characteristics have not been used in calibration. The time-mean spatial patterns of ϕ at the test glacier are well-reproduced (Fig. 2a, 2b). The RMSE is low throughout the domain (Fig. 2c), except on a small portion near the glacier terminus. The time series shown in Figure 2d demonstrate that the ANN performance in reproducing temporal dynamics at seasonal and inter-annual scales are similar to its performance on calibration glaciers (compare with Fig. 1d). Here also, the orange lines in Fig. 2d show a time series corresponding to a low-performance location. Again, the ANN still captures temporal dynamics correctly, but has a consistent bias over the time series at this location. Finally, the metrics of performance for this test glacier show an RMSE lower than 0.56 MPa, a small positive bias of 0.24 MPa, and $R^2 > 0.96$.

171

3.3 Sensitivity to number of calibration years

172

173

174

175

176

177

To calibrate the ANN, we have used 30 years (1975-2004) of GlaDS output at the calibration glaciers, and preserved 5 years (2005-2009) of output for testing (see Supporting Information). In this section, we investigate the sensitivity of ANN accuracy to the number of calibration years. Starting with all 30 years of available GlaDS output, we reduce the calibration data by 3-year increments, re-train the ANN at each increment, and evaluate performance metrics always on the 2005-2009 years.

178

179

180

Figure 3a shows the ratios in the R^2 , RMSE and absolute bias metrics for each sensitivity experiment, with respect to the results computed when all the 30 calibration years are used in the ANN calibration. There is no decrease in accuracy for calibration data

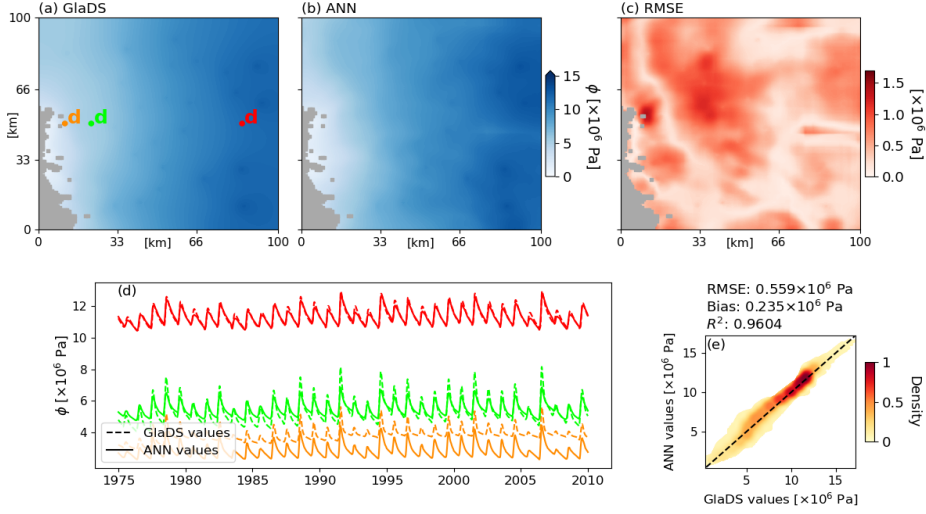


Figure 2. Spatial generalization performance of the ANN. Maps of mean 1975-2009 ϕ fields at the test glacier (Upernavik, Fig. S1 for location) simulated by (a) GlaDS, and (b) the ANN. The Root-Mean-Square Error (RMSE) of the ANN with respect to GlaDS is shown in (c). Time series (d) of ϕ at specific grid points simulated by GlaDS (dashed lines) and the ANN (solid lines), with color-coded locations shown in (a). Performance statistics (e) of the ANN with respect to GlaDS evaluated at all the grid points of the test glacier for all the 1975-2009 time steps.

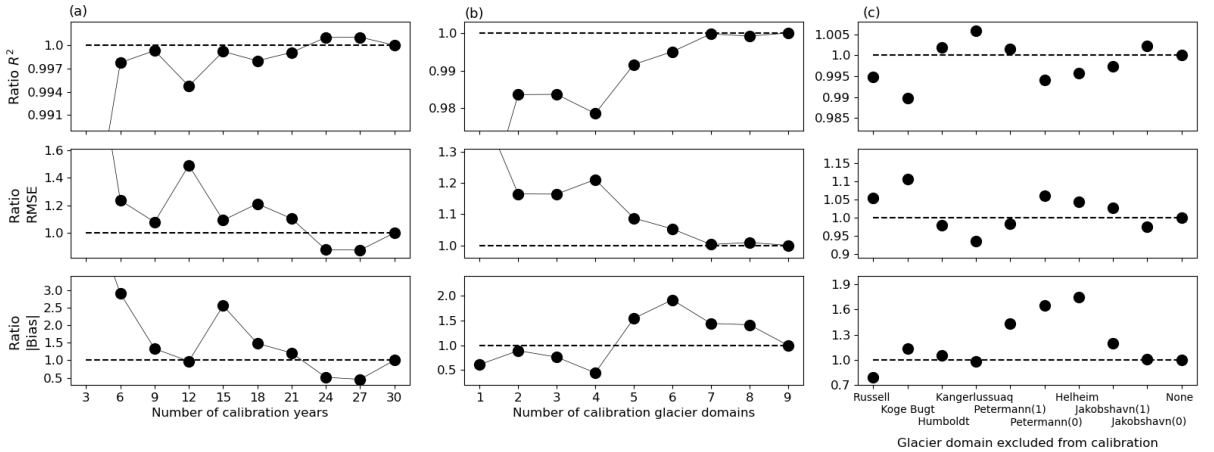


Figure 3. Sensitivity experiments (a) for number of years included in the calibration data, with evaluation on the 2005-2009 test years. Sensitivity experiments (b) for number of glacier domains included in the calibration data, with evaluation on the test Upernavik glacier domain. Leave-one-out experiments (c) in which each calibration glacier domain is separately excluded from the calibration data, with evaluation on the test Upernavik glacier domain. Dashed lines show no performance change with respect to the model calibrated with the default calibration data (30,9,'None' in a,b,c).

181 reduced down to 21 years. Small accuracy variations down to this limit are likely due
 182 to the inherent randomness in the training procedure of neural networks, through the
 183 parameter initialization method and the optimization algorithm. If calibration years are
 184 reduced to 18 years or less, performance metrics decrease and show more volatility. RMSE
 185 is increased by 21 % for 18 years, and by >250% for <6 years of calibration data.

186 3.4 Sensitivity to number of calibration glaciers

187 We also perform a sensitivity analysis to the number of glacier domains included
 188 in the calibration. Our initial calibration data set consists of seven glaciers, two of which
 189 have been split in two to match with the ANN domain input size, thus resulting in nine
 190 distinct glacier domains for calibration (see Supporting Information). Here, we sequen-
 191 tially drop one additional random glacier domain from the calibration data, and evalu-
 192 ate the ANN performance metrics always on the same test glacier (Upernavik).

193 Figure 3b shows the sensitivity of the performance metrics to the number of cal-
 194 ibration glaciers. Accuracy decrease is minor when the calibration data are reduced to
 195 8 and 7 domains, except for increases in the absolute bias. However, we observe a strong
 196 deterioration in accuracy for calibration data sets of 6 or fewer glacier domains. At 4 do-
 197 mains, the increase in RMSE reaches 21%. The ANN accuracy has levelled off for >6
 198 glacier domains, showing that we have used sufficient calibration data.

199 Finally, we investigate if any single glacier domain is disproportionately important
 200 to the ANN accuracy at the test glacier. We repeat the ANN training with each one of
 201 the 9 calibration glacier domains left out of the calibration data, and then evaluate per-
 202 formance metrics on the test glacier (Fig. 3c). In agreement with the results from ex-
 203 cluding only a single glacier domain shown above, changes in performance metrics are
 204 mostly small. For some of these leave-one-out experiments, performance metrics even
 205 improve slightly. The maximal increase in RMSE is 10.6 %, occurring when Koge Bugt
 206 glacier is left out (Fig. 3c). These results show that the ANN calibration is not exces-
 207 sively sensitive to any particular glacier. This verifies that the ANN does not predict at
 208 an out-of-sample glacier based only on the characteristics from the most similar glacier
 209 seen in training, but rather that it learns general relationships controlling ϕ patterns across
 210 different glaciological contexts.

211 3.5 Ice sheet model forcing

212 We now demonstrate that our ANN emulator can readily be used as forcing for an
 213 ice sheet model. We run the Ice-sheet and Sea-level System Model (Larour et al., 2012)
 214 at the test glacier of our data set: Upernavik (see Supporting Information for simula-
 215 tion details). We perform two 1975-2009 simulations: one forced with p_w from GlaDS
 216 output (GlaDS-forced run), and the other with p_w from the ANN (ANN-forced run). Ex-
 217 cept for the p_w forcing, the two simulations share identical initial conditions, climatic
 218 forcing, and other parameterizations, thus isolating differences in ice thickness and ice
 219 flow caused by discrepancies in the ANN emulation of GlaDS.

220 Figures 4a and 4b show the change in ice thickness (ΔH_{ice}) over the 35 years of
 221 simulations for the GlaDS-forced and ANN-forced runs, respectively. The patterns of ΔH_{ice}
 222 are very close between these two runs, which is confirmed at a grid point level (Fig. 4c,
 223 $R^2=0.88$). To quantify ice flow variability, we compute the temporal standard deviation
 224 in ice velocity ($\sigma(u_{ice})$) at each grid point. For this metric also, the GlaDS-forced and
 225 ANN-forced runs are in close agreement throughout the domain (Fig. 4d, 4e). However,
 226 $\sigma(u_{ice})$ is slightly underestimated by the ANN-forced run at the glacier terminus, espe-
 227 cially at the northernmost branch where we observed the modest bias on ϕ of the ANN
 228 (Fig. 2c, 2d). At the two other branches, $\sigma(u_{ice})$ in our two simulations agree well. Through-
 229 out the domain, the ANN-forced run explains 78% of the variance in $\sigma(u_{ice})$ of the GlaDS-

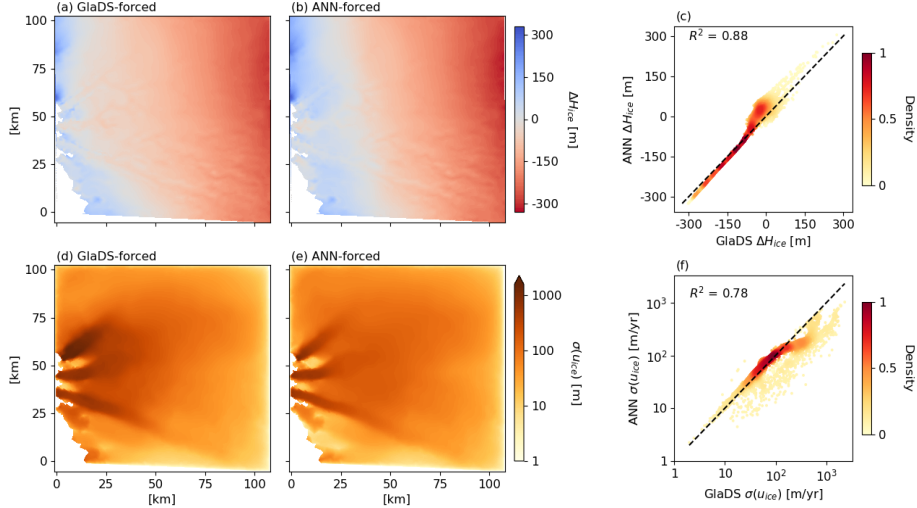


Figure 4. Results of 1975-2009 ice sheet model runs at the test glacier (Upernavik), with subglacial hydrology forcing from GlaDS (a,d) and from the ANN (b,e). Maps show ice thickness change (a,b, variable ΔH_{ice}), and standard deviation in ice velocities (d,e, variable $\sigma(u_{ice})$) over 1975-2009. Performance of the ANN-forced run with respect to the GlaDS-forced run in ΔH_{ice} (c) and $\sigma(u_{ice})$ (f). Note the logarithmic colorbar in (d,e) and axes in (f).

230 forced run (evaluated on logarithmic scale). The previous sections demonstrated the high
 231 accuracy of the ANN in reproducing ϕ spatio-temporal evolution as modeled by GlaDS.
 232 This section shows that this accuracy translates into dynamical ice sheet model results
 233 being only weakly sensitive to substituting our ANN for GlaDS to prescribe the p_w forc-
 234 ing.

235 In terms of computation, savings are large: simulating the 1975-2009 period in GlaDS
 236 over the Upernavik domain requires 859.9 CPU-hours, compared to 1.0 CPU-hour for
 237 predictions from our ANN on an identical core, i.e., close to $\mathcal{O}(10^3)$ faster. Finally, the
 238 35-year GlaDS simulation required 268 times more CPU-hours than the ice sheet model
 239 simulation itself (3.2 CPU-hours), showing that subglacial hydrology models are a ma-
 240 jor computational bottleneck for large-scale ice sheet simulations.

241 4 Discussion

242 Our ANN produces realistic spatio-temporal patterns of subglacial hydraulic po-
 243 tential. It is skillful at temporal and spatial generalization on out-of-sample cases, when
 244 trained on as few as seven glacier domains and two decades of data. We do find small
 245 discrepancies between the ANN and GlaDS ϕ outputs, typically ranging between 0.2 and
 246 1.5 MPa. Such values are smaller than discrepancies between subglacial hydrology mod-
 247 els calculated in a recent intercomparison study (de Fleurian et al., 2018). Note that this
 248 comparison is not exact, because the intercomparisons used idealized configurations, whereas
 249 we use realistic Greenland glacier configurations. Still, because subglacial hydrology mod-
 250 els are themselves an imperfect representation of real subglacial hydrology, the ANN out-
 251 put falling within typical inter-model spread reinforces our confidence that the ANN per-
 252 forms similarly to state-of-the-art numerical models.

253 Despite the demonstrated generalization capabilities of our ANN, we emphasize that
 254 deep learning models are prone to large errors, and possibly implausible behavior, when

used to extrapolate beyond their range of training conditions (Rasp et al., 2018; Reichstein et al., 2019). Training data should encompass the range of meltwater runoff and glaciological conditions that will be targeted for predictions of the subglacial hydrology deep learning model. For future Greenland ice sheet projections, training should include high-runoff forcing, as surface melting is predicted to increase (Fettweis et al., 2013). We have verified the quality of our ANN training through sensitivity analyses, demonstrating that calibration data are sufficient, and that the ANN does not overfit but has learned general spatio-temporal relationships inherent to subglacial hydrology.

The ANN presented in this study, and machine learning techniques more generally, provide solutions to the extreme computational expense of running subglacial hydrology models in realistic ice sheet simulations. In addition to subglacial hydrology, machine learning techniques could also potentially replace other inaccurate parameterizations of ice sheet processes, where sufficient observations and/or high-fidelity model output exist to use as training data. For example, the physics of iceberg calving remain challenging to simulate, but capturing observed temporal dynamics of calving rates could be the target of machine learning parameterizations. As another example, such parameterizations can aim to represent ice sheet surface mass balance at fine scales without the need for expensive climate model downscaling, as has already been demonstrated for Alpine glaciers (Bolibar et al., 2020) and for the Antarctic Peninsula (van der Meer et al., 2023).

Observations of subglacial water pressure are scarce, especially when considering the large data requirements for deep learning. Thus, our emulator has been calibrated exclusively with output from high-fidelity models, which may themselves be biased. The value of observations could be exploited through pre-training on model output followed by fine-tuning on existing, spatio-temporally sparse observations (e.g., Rasp & Thuerey, 2020). In addition, there are other possible future avenues for improving this deep learning emulator. Associating the convolutional nature of our ANN with recurrent neural networks would allow to simulate temporal dependencies explicitly, in addition to spatial patterns. Temporal dependencies are here accounted for in an ad-hoc manner through our processing of inputs (see Supporting Information). Also, here the coupling of the ANN and the ice sheet model is one-way; the ANN is run first, and its output used as forcing to the ice sheet model. This approach allows the subglacial hydrology emulator to be used directly with any ice sheet model. Tight two-way coupling would capture feedback processes between subglacial hydrology and changes in ice sheet geometry and velocities, but requires implementation of the ANN within the source code of an ice sheet model. The lack of deep learning libraries in low-level languages, which are the basis of most modern ice sheet and climate model architectures, makes such implementation challenging (Partee et al., 2022). Recent development of new ice sheet models within high-level languages (e.g., Shapero et al., 2021) hold promise for better integration of machine learning directly into ice sheet models.

5 Conclusion

Our study demonstrates that deep learning techniques enable simulation of subglacial hydrology for ice sheet model forcing. Our emulator reproduces output of a state-of-the-art subglacial hydrology model with great fidelity, strong generalization skills, and $\mathcal{O}(10^3)$ savings in computation time. This advance has the potential to enable coupled simulations of ice sheet flow and evolving subglacial hydrology over entire ice sheets on centennial and longer time scales. Our work also demonstrates how machine learning techniques can be adopted in the ice sheet modeling community to resolve current issues related to knowledge gaps and computational bottlenecks. This general methodology is not limited to emulating subglacial hydrology models, but can potentially improve the representation of many other ice sheet model processes. Recent advances in computa-

306 tional capabilities and machine learning will, in parallel with traditional ice sheet model
 307 development, bring key improvements in predictions of ice sheet response to climate change.

308 6 Open Research

309 Model code is openly available at: <https://doi.org/10.5281/zenodo.8006962>

310 The code includes all scripts to run GlaDS, to process data, to train the ANN, and
 311 to predict with the ANN. The input files, hydrology model results, trained ANN param-
 312 eter files, and final ANN predictions at the 8 glaciers of this study are included. Detailed
 313 data and code descriptions are provided.

314 Acknowledgments

315 VV was funded by the Heising-Simons Foundation (Grant 2020-1965). Computing re-
 316 sources were provided by the Partnership for an Advanced Computing Environment (PACE)
 317 at the Georgia Institute of Technology, Atlanta. The authors thank Mathieu Morlighem
 318 and Shivani Ehrenfeucht for advice about GlaDS.

319 References

- 320 Bartholomew, I. D., Nienow, P., Sole, A. J., Mair, D. W. F., Cowton, T. R., Palmer,
 321 S. J., & Wadham, J. L. (2011). Supraglacial forcing of subglacial drainage in
 322 the ablation zone of the greenland ice sheet. *Geophysical Research Letters*, *38*.
 323 Bolibar, J., Rabatel, A., Gouttevin, I., Galiez, C., Condom, T., & Sauquet, E.
 324 (2020). Deep learning applied to glacier evolution modelling. *The Cryosphere*.
 325 Brenowitz, N. D., & Bretherton, C. S. (2018). Prognostic validation of a neural net-
 326 work unified physics parameterization. *Geophysical Research Letters*, *45*, 6289
 327 - 6298.
 328 Brinkerhoff, D. J., Aschwanden, A., & Fahnestock, M. A. (2021). Constraining
 329 subglacial processes from surface velocity observations using surrogate-based
 330 bayesian inference. *Journal of Glaciology*, *67*, 385 - 403.
 331 Budd, W. F., Jenssen, D., & Smith, I. N. (1984). A three-dimensional time-
 332 dependent model of the west antarctic ice sheet. *Annals of Glaciology*, *5*,
 333 29 - 36.
 334 Cowton, T. R., Nienow, P., Sole, A. J., Wadham, J. L., Lis, G., Bartholomew, I. D.,
 335 ... Chandler, D. (2013). Evolution of drainage system morphology at a land-
 336 terminating greenlandic outlet glacier. *Journal of Geophysical Research: Earth*
 337 *Surface*, *118*, 29 - 41.
 338 de Fleurian, B., Werder, M. A., Beyer, S., Brinkerhoff, D. J., Delaney, I., Dow,
 339 C. F., ... Sommers, A. N. (2018). Shmip the subglacial hydrology model
 340 intercomparison project. *Journal of Glaciology*, *64*, 897 - 916.
 341 Ehrenfeucht, S., Morlighem, M., Rignot, E., Dow, C. F., & Mouginot, J. (2022).
 342 Seasonal acceleration of petermann glacier, greenland, from changes in sub-
 343 glacial hydrology. *Geophysical Research Letters*, *50*.
 344 Fettweis, X., Box, J. E., Agosta, C., Amory, C., Kittel, C., Lang, C., ... Gallée, H.
 345 (2016). Reconstructions of the 1900–2015 greenland ice sheet surface mass bal-
 346 ance using the regional climate mar model. *The Cryosphere*, *11*, 1015-1033.
 347 Fettweis, X., Franco, B., Tedesco, M., van Angelen, J. H., Lenaerts, J. T. M.,
 348 van den Broeke, M., & Gallée, H. (2013). Estimating the greenland ice sheet
 349 surface mass balance contribution to future sea level rise using the regional
 350 atmospheric climate model mar. *The Cryosphere*, *7*, 469-489.
 351 Goelzer, H., Nowicki, S. M. J., Payne, A. J., Larour, E. Y., Seroussi, H., Lipscomb,
 352 W. H., ... van den Broeke, M. R. (2020). The future sea-level contribu-
 353 tion of the greenland ice sheet: a multi-model ensemble study of ismip6. *The*
 354 *Cryosphere*.

- 355 He, K., Zhang, X., Ren, S., & Sun, J. (2015). Delving deep into rectifiers: Surpassing
356 human-level performance on imagenet classification. *2015 IEEE International
357 Conference on Computer Vision (ICCV)*, 1026-1034.
- 358 Hewitt, I. J. (2013). Seasonal changes in ice sheet motion due to melt water lubrication.
359 *Earth and Planetary Science Letters*, *371*, 16-25.
- 360 Hoffman, M. J., Andrews, L. C., Price, S. A., Catania, G. A., Neumann, T. A.,
361 Lüthi, M. P., ... Morriss, B. F. (2016). Greenland subglacial drainage evolution
362 regulated by weakly connected regions of the bed. *Nature Communications*, *7*.
- 363
- 364 Hornik, K., Stinchcombe, M. B., & White, H. L. (1989). Multilayer feedforward networks
365 are universal approximators. *Neural Networks*, *2*, 359-366.
- 366 Joughin, I. R., Smith, B. E., & Howat, I. M. (2017). A complete map of greenland
367 ice velocity derived from satellite data collected over 20 years. *Journal of
368 Glaciology*, *64*, 1 - 11.
- 369 Jouvett, G., Cordonnier, G., Kim, B., Lüthi, M. P., Vieli, A., & Aschwanden, A.
370 (2021). Deep learning speeds up ice flow modelling by several orders of magni-
371 tude. *Journal of Glaciology*, *68*, 651 - 664.
- 372 Kazmierczak, E., Sun, S., Coulon, V., & Pattyn, F. (2022). Subglacial hydrology
373 modulates basal sliding response of the antarctic ice sheet to climate forcing.
374 *The Cryosphere*.
- 375 King, M. D., Howat, I. M., Candela, S. G., Noh, M.-J., Jeong, S., Noël, B. P. Y., ...
376 Negrete, A. (2020). Dynamic ice loss from the greenland ice sheet driven by
377 sustained glacier retreat. *Communications Earth & Environment*, *1*.
- 378 Kingma, D. P., & Ba, J. (2014). Adam: A method for stochastic optimization.
379 *CoRR*, *abs/1412.6980*.
- 380 Krebs-Kanzow, U., Gierz, P., Rodehacke, C. B., Xu, S., Yang, H., & Lohmann, G.
381 (2020). The diurnal energy balance model (debm): a convenient surface mass
382 balance solution for ice sheets in earth system modeling. *The Cryosphere*, *15*,
383 2295-2313.
- 384 Lakshminarayanan, B., Pritzel, A., & Blundell, C. (2016). Simple and scalable pre-
385 dictive uncertainty estimation using deep ensembles. In *Nips*.
- 386 Larour, E. Y., Seroussi, H., Morlighem, M., & Rignot, E. (2012). Continental
387 scale, high order, high spatial resolution, ice sheet modeling using the ice sheet
388 system model (issm). *Journal of Geophysical Research*, *117*.
- 389 LeCun, Y., Bengio, Y., & Hinton, G. (2015). Deep learning. *Nature*, *521*, 436-444.
- 390 Lemley, J., Bazrafkan, S., & Corcoran, P. M. (2017). Smart augmentation learning
391 an optimal data augmentation strategy. *IEEE Access*, *5*, 5858-5869.
- 392 Morlighem, M., Williams, C. N., Rignot, E., An, L., Arndt, J. E., Bamber, J. L., ...
393 Zinglensen, K. B. (2017). Bedmachine v3: Complete bed topography and ocean
394 bathymetry mapping of greenland from multibeam echo sounding combined
395 with mass conservation. *Geophysical Research Letters*, *44*, 11051 - 11061.
- 396 Nienow, P., Sole, A. J., Slater, D. A., & Cowton, T. R. (2017). Recent advances in
397 our understanding of the role of meltwater in the greenland ice sheet system.
398 *Current Climate Change Reports*, *3*, 330-344.
- 399 Ootosaka, I. N., Shepherd, A., Ivins, E. R., Schlegel, N., Amory, C., van den Broeke,
400 M. R., ... Wouters, B. (2023). Mass balance of the greenland and antarctic ice
401 sheets from 1992 to 2020. *Earth System Science Data*.
- 402 Partee, S., Ellis, M. S., Rigazzi, A., Shao, A. E., Bachman, S. D., Marques, G., &
403 Robbins, B. (2022). Using machine learning at scale in numerical simulations
404 with smartsim: An application to ocean climate modeling. *J. Comput. Sci.*,
405 *62*, 101707.
- 406 Paszke, A., Gross, S., Massa, F., Lerer, A., Bradbury, J., Chanan, G., ... Chintala,
407 S. (2019). Pytorch: An imperative style, high-performance deep learning
408 library. In *Neural information processing systems*.
- 409 Rasp, S., Pritchard, M. S., & Gentine, P. (2018). Deep learning to represent subgrid

- 410 processes in climate models. *Proceedings of the National Academy of Sciences*
 411 *of the United States of America*, 115, 9684 - 9689.
- 412 Rasp, S., & Thuerey, N. (2020). Data-driven medium-range weather prediction with
 413 a resnet pretrained on climate simulations: A new model for weatherbench.
 414 *Journal of Advances in Modeling Earth Systems*, 13.
- 415 Reichstein, M., Camps-Valls, G., Stevens, B., Jung, M., Denzler, J., Carvalhais, N.,
 416 & Prabhat. (2019). Deep learning and process understanding for data-driven
 417 earth system science. *Nature*, 566, 195-204.
- 418 Ronneberger, O., Fischer, P., & Brox, T. (2015). U-net: Convolutional networks for
 419 biomedical image segmentation. *ArXiv, abs/1505.04597*.
- 420 Schoof, C. (2010). Ice-sheet acceleration driven by melt supply variability. *Nature*,
 421 468, 803-806.
- 422 Seroussi, H., Nowicki, S. M. J., Payne, A. J., Goelzer, H., Lipscomb, W. H., Abe-
 423 Ouchi, A., ... Zwinger, T. (2020). Ismip6 antarctica: a multi-model ensemble
 424 of the antarctic ice sheet evolution over the 21st century. *The Cryosphere*.
- 425 Shapero, D., Badgley, J. A., Hoffmann, A., & Joughin, I. R. (2021). icepack: a new
 426 glacier flow modeling package in python, version 1.0. *Geoscientific Model De-*
 427 *velopment*.
- 428 Shepherd, A., Hubbard, A., Nienow, P., King, M. A., McMillan, M., & Joughin,
 429 I. R. (2009). Greenland ice sheet motion coupled with daily melting in late
 430 summer. *Geophysical Research Letters*, 36.
- 431 Siu, K. (2022). Modelling subglacial hydrology under future climate scenarios in
 432 wilkes subglacial basin, antarctica..
- 433 Smith, L. C., Andrews, L. C., Pitcher, L. H., Overstreet, B. T., Rennermalm, Å. K.,
 434 Cooper, M. G., ... Simpson, C. E. (2021). Supraglacial river forcing of sub-
 435 glacial water storage and diurnal ice sheet motion. *Geophysical Research*
 436 *Letters*, 48.
- 437 van der Meer, M., de Roda Husman, S., & Lhermitte, S. (2023). Deep learning
 438 regional climate model emulators: A comparison of two downscaling train-
 439 ing frameworks. *Journal of Advances in Modeling Earth Systems*, 15(6),
 440 e2022MS003593. Retrieved from [https://agupubs.onlinelibrary.wiley](https://agupubs.onlinelibrary.wiley.com/doi/abs/10.1029/2022MS003593)
 441 [.com/doi/abs/10.1029/2022MS003593](https://doi.org/10.1029/2022MS003593) (e2022MS003593 2022MS003593) doi:
 442 <https://doi.org/10.1029/2022MS003593>
- 443 van de Wal, R., Smeets, C. J. P. P., Boot, W., Stoffelen, M., van Kampen, R.,
 444 Doyle, S. H., ... Hubbard, A. (2015). Self-regulation of ice flow varies across
 445 the ablation area in south-west greenland. *The Cryosphere*, 9, 603-611.
- 446 Werder, M. A., Hewitt, I. J., Schoof, C., & Flowers, G. E. (2013). Modeling chan-
 447 nelized and distributed subglacial drainage in two dimensions. *Journal of Geo-*
 448 *physical Research: Earth Surface*, 118, 2140 - 2158.
- 449 Zwally, H. J., Abdalati, W., Herring, T. A., Larson, K. M., Saba, J. L., & Steffen, K.
 450 (2002). Surface melt-induced acceleration of greenland ice-sheet flow. *Science*,
 451 297, 218 - 222.